Optical Materials 48 (2015) 252–257

Contents lists available at ScienceDirect

Optical Materials

journal homepage: www.elsevier.com/locate/optmat

Energy transfer processes in $Ca_3Tb_{2-x}Eu_xSi_3O_{12}$ ($x = 0–2$)

I. Carrasco [a,*], K. Bartosiewicz [b,c], M. Nikl [b], F. Piccinelli [a], M. Bettinelli [a]

[a] Luminescent Materials Laboratory, Dept. of Biotechnology, University of Verona, Strada Le Grazie 15, 37134 Verona, Italy
[b] Dept. Optical Materials, Institute of Physics AS CR, Cukrovarnicka 10, Praha, Czech Republic
[c] Faculty of Nuclear Sciences and Physical Engineering, Czech Technical University in Prague, Brehova 7, Praha 1, 11519, Czech Republic

ARTICLE INFO

Article history:
Received 12 June 2015
Received in revised form 29 July 2015
Accepted 11 August 2015

Keywords:
Phosphors
Silico-carnotite
Luminescence
Energy transfer

ABSTRACT

The luminescent properties of Tb^{3+} and Eu^{3+} have been studied in several silicates having a silico-carnotite-type structure. Fast energy migration among Tb^{3+} ions has been found in $Ca_3Tb_2Si_3O_{12}$ and $Ca_3Tb_{2-x}Eu_xSi_3O_{12}$ ($x = 0–0.1$). In the case of $Ca_3Tb_{2-x}Eu_xSi_3O_{12}$, Tb^{3+}–Eu^{3+} energy transfer is observed upon excitation in the UV bands of Tb^{3+}. The transfer gives rise to strong emission from Eu^{3+} in the red spectral region at 612 nm. The efficiency of the transfer at room temperature in $Ca_3Tb_{1.9}Eu_{0.1}Si_3O_{12}$ has been evaluated. The temperature evolution of the luminescent properties of $Ca_3Tb_2Si_3O_{12}$ and $Ca_3Tb_{1.9}Eu_{0.1}Si_3O_{12}$ has been studied at temperatures ranging from 8 to 330 K.

1. Introduction

Despite numerous studies over the years, energy transfer processes are still interesting from both a fundamental and an applied point of view, as transfer processes in pairs of ions and from the host to luminescent ions are crucial for development of innovative phosphors, scintillators and materials for solar cells [1,2]. For this reason, it is interesting to consider sensitization process, which is a traditional manner for enhancing luminescence efficiency of phosphors, taking into account the increasing importance of efficient VUV (~145–190 nm) excited phosphors, essential to plasma display panels [3], or near UV-LEDs (~370 nm) excited phosphors, given their potential application in the development of white LEDs [4]. It is well known that Tb^{3+} is a sensitizer for Eu^{3+} in the UV/VIS range [5,6] but also in the VUV [1], making the materials containing Tb^{3+} and Eu^{3+} an interesting field in the search for novel efficient phosphors [7,8].

Among the large number of suitable hosts for Ln^{3+} luminescent ions, silicate compounds play an important role due to their good transparency in the UV/VIS region, chemical stability and relatively low price. Silicates $Ca_3M_2Si_3O_{12}$ ($M = Ln^{3+}$) exhibit a stable silico carnotite-like structure when M is a lanthanide ion in the range Eu–Lu [9]. These materials are of high interest from the spectroscopic point of view, and are to be considered as efficient hosts for doping with luminescent trivalent lanthanide ions [10].

In this work, the Tb^{3+}–Eu^{3+} energy transfer processes have been analyzed by systematically studying the room temperature luminescent properties of $Ca_3Tb_2Si_3O_{12}$, $Ca_3Eu_2Si_3O_{12}$ and $Ca_3Tb_{2-x}Eu_xSi_3O_{12}$ powders for various Eu^{3+} doping concentration, as well as the evolution with temperature of the luminescent properties of $Ca_3Tb_2Si_3O_{12}$ and $Ca_3Tb_{1.9}Eu_{0.1}Si_3O_{12}$ powders.

2. Experimental methods and structural characterization

Polycrystaline samples of $Ca_3Tb_2Si_3O_{12}$, $Ca_3Tb_{2-x}Eu_xSi_3O_{12}$ ($x = 0.02$, 0.04, 0.08 and 0.1) and $Ca_3Eu_2Si_3O_{12}$ have been obtained by solid state reaction at high temperature. $CaCO_3$ (>99%), Tb_4O_7 (99.99%), SiO_2 (99.999%) and Eu_2O_3 (99.99%) powders were mixed and pressed into pellets under a load of 10 tons. The samples underwent three thermal treatments at 1450 °C for 3 h under air atmosphere, with intermediate grindings.

Powder X-ray diffraction (XRD) measurements were performed to analyze the structure of the synthesized compounds. Experiments were carried out with a Thermo ARL XTRA powder diffractometer, operating in the Bragg-Brentano geometry and equipped with a Cu-anode X-ray source (Kα, $\alpha = 1.5418$ Å), using a Peltier Si (Li) cooled solid state detector. The patterns were collected with a scan rate of 0.04°/s in the 5–90° 2θ range. The phase identification was performed with the PDF-4+2013 database provided by the International Centre for Diffraction Data (ICDD). Polycrystalline samples were ground in a mortar and then put in a low-background sample holder for the data collection. All the obtained materials are single phase and posses an orthorhombic crystal structure (space group, *Pnma*). They are isostructural with

* Corresponding author.
E-mail address: irene.carrascoruiz@univr.it (I. Carrasco).

http://dx.doi.org/10.1016/j.optmat.2015.08.009
0925-3467/

silico-carnotite $Ca_5(PO_4)_2SiO_4$ (orthorhombic) [11]. The structural formula can be represented as $AB_2C_2(EO_4)_3$ where A, B and C refer, respectively, to nine-,eight-, and seven-coordinate cationic sites, characterized by very low site symmetries (C_1 or C_s). In the case of $Ca_3Ln_2Si_3O_{12}$ the distribution of the cations on the three available crystal sites is strongly dependent on the nature of the rare earth ion [12,13].

Room temperature luminescence was measured with a Fluorolog 3 (Horiba-Jobin Yvon) spectrofluorometer, equipped with a Xe lamp, a double excitation monochromator, a single emission monochromator (mod.HR320) and a photomultiplier in photon counting mode for the detection of the emitted signal. For the temperature dependent study, the luminescence and decay kinetics measurements were performed in the temperature range 8–330 K using the custom made 5000 M Horiba Jobin Yvon fluorescence spectrometer. Janis closed cycle cryostat was used in all the experiments. In the steady state spectra measurements, the sample was excited by deuterium lamp (Heraus Gmbh). All the spectra were corrected for the spectral distortions of the setup. In decay kinetics measurements a xenon microsecond flashlamp was used and the signal was recorded by means of multichannel scaling method. True decay times were obtained using the convolution of the instrumental response function with an exponential function and the least-square-sum-based fitting program (SpectraSolve software package).

3. Results and discussion

3.1. Room temperature spectroscopy

Fig. 1 shows the room temperature emission spectra of $Ca_3Tb_2Si_3O_{12}$ measured upon excitation at 377 nm (in $^5D_3$ level of Tb^{3+}) and emission spectrum of $Ca_3Eu_2Si_3O_{12}$ recorded upon excitation at 393 nm. For $Ca_3Tb_2Si_3O_{12}$ it is possible to observe strong $^5D_4$ emission and no significant $^5D_3$ emission, due to efficient cross relaxation processes expected in fully concentrated Tb^{3+} materials. These processes transfer population from $^5D_3$ to $^5D_4$, strongly reducing the $^5D_3$ lifetime and the blue luminescence intensity with the increase of Tb^{3+} concentration [14,15]. In the case of $Ca_3Eu_2Si_3O_{12}$ five bands corresponding to emission from $^5D_0$ level of Eu^{3+} are observed. Emission spectra of $Ca_3Tb_{2-x}Eu_xSi_3O_{12}$ (x = 0.02, 0.04, 0.08 and 0.1) measured upon excitation at 377 nm are also shown in Fig. 1. For these materials the spectra are dominated by strong bands originating from the $^5D_0$ level of Eu^{3+}, and only weak $^5D_4$–$^7F_6$ and $^5D_4$–$^7F_5$ Tb^{3+} emission bands are observed. These features clearly indicate the existence of an energy transfer process from Tb^{3+} to Eu^{3+}. For all the compounds, emission bands are relatively broad due to the high degree of disorder present in the host, as discussed by Blasse [16]. Inset of Fig. 1 presents in detail Tb^{3+} emission bands for Eu-doped compounds. Spectra are normalized to the $^5D_0$–$^7F_2$ band of Eu^{3+}. It is noticeable that the higher the Eu^{3+} concentration, the lower the intensity of Tb^{3+} emission bands. No Tb^{3+} emission has been observed when directly exciting into Eu^{3+} at 393 nm, confirming that no back transfer is present in the system.

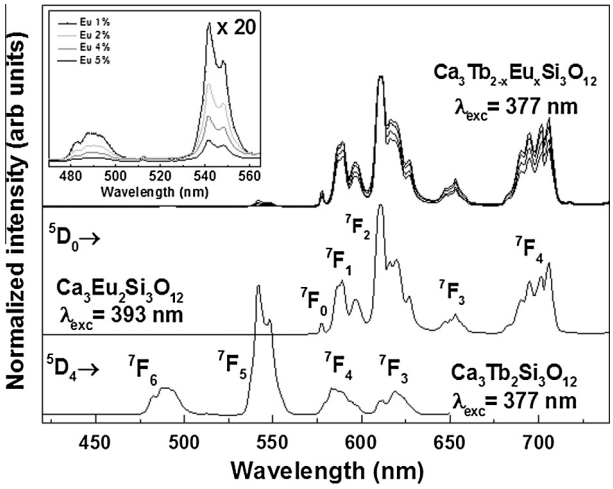

Fig. 1. Room temperature emission spectra of $Ca_3Tb_2Si_3O_{12}$, $Ca_3Eu_2Si_3O_{12}$ and $Ca_3Tb_{2-x}Eu_xSi_3O_{12}$ measured upon excitation at 377, 377 and 393 nm respectively. The spectrum of $Ca_3Tb_2Si_3O_{12}$ is normalized to Tb^{3+} $^5D_4$–$^7F_5$ emission, whereas the spectra of $Ca_3Eu_2Si_3O_{12}$ and $Ca_3Tb_{2-x}Eu_xSi_3O_{12}$ are normalized to Eu^{3+} $^5D_0$–$^7F_2$ emission. Inset shows in detail the weak Tb^{3+} emission bands for $Ca_3Tb_{2-x}Eu_xSi_3O_{12}$.

The excitation spectra of all samples are shown in Fig. 2. The energy level diagrams for Tb^{3+} and Eu^{3+} in the $Ca_3Tb_2Si_3O_{12}$:Eu phosphors. are presented in Fig. 3 to help comprehension of the system. In the case of $Ca_3Tb_2Si_3O_{12}$ the spectrum is composed of overlapping bands in the UV ranging from 300 nm to almost 400 nm, and a weaker band at 480 nm. The transitions have been designated as $^7F_6$–$^5G_3$ at 340 nm, $^7F_6$–$^5L_8 + {}^5G_4$ at 350 nm, $^7F_6$–$^5D_3$ at377 nm, which is the most intense, and $^7F_6$–$^5D_4$ at 480 nm. The spectrum of $Ca_3Eu_2Si_3O_{12}$ is composed of various bands ranging from 360 nm to 430 nm and other bands at 460 nm and 530 nm. In this case the transitions have been assigned as $^7F_0$–$^5D_4$ at 360 nm, $^7F_0$–$^5L_7$ at 393 nm, which is the most intense, $^7F_0$–$^5D_3$ at 412 nm, $^7F_0$–$^5D_2$ at 460 nm, $^7F_0$–$^5D_1$ at 525 nm and $^7F_1$–$^5D_1$ at 530 nm. In the case of Eu-doped samples, the excitation spectra when monitoring the $^5D_0$ emission of Eu^{3+} are dominated by Tb^{3+} bands in the UV region. Only a few Eu^{3+} excitation bands are observed. These results confirm the Tb^{3+}–Eu^{3+} energy transfer. Various Tb^{3+}–Eu^{3+} phonon assisted energy transfer processes have been proposed in the literature [5,17]; some of the most important are:

$$Tb^{3+}(^5D_4) + Eu^{3+}(^7F_0) + \Delta E_{ph} \rightarrow Tb^{3+}(^7F_4) + Eu^{3+}(^5D_0)$$

$$Tb^{3+}(^5D_3) + Eu^{3+}(^7F_0) \rightarrow Tb^{3+}(^7F_3) + Eu^{3+}(^5D_2) + \Delta E_{ph}$$

where the phonon energies involved (ΔE_{ph}) are relatively low (less than 500 cm^{-1}). Due to fast multiphonon relaxation in the host, energy transfer will lead in all cases only to emission from $^5D_0$, as discussed by Bettinelli et al. [6].

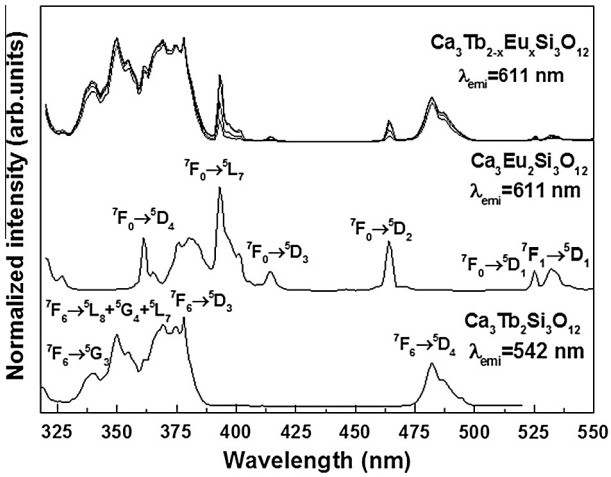

Fig. 2. Room temperature excitation spectra of $Ca_3Tb_2Si_3O_{12}$, $Ca_3Eu_2Si_3O_{12}$ and $Ca_3Tb_{2-x}Eu_xSi_3O_{12}$ monitoring emission at 542 nm (Tb^{3+}), 611 nm (Eu^{3+}) and 611 nm (Eu^{3+}) respectively.

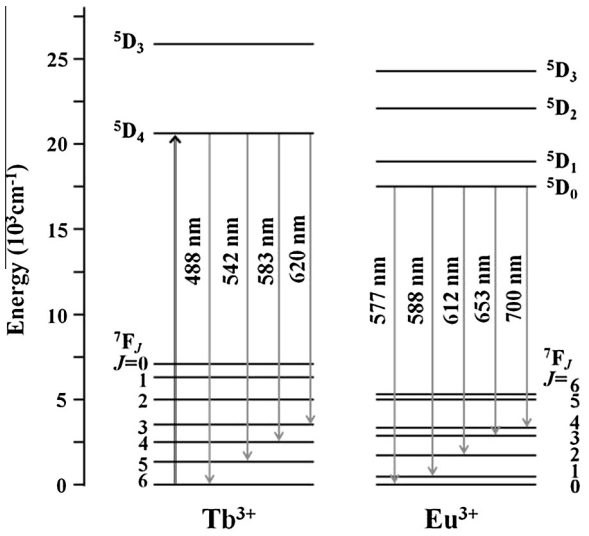

Fig. 3. Energy level diagram for Tb^{3+} and Eu^{3+} ions in $Ca_3Tb_2Si_3O_{12}$: Eu phosphors.

Decay curves for Tb^{3+} and Eu^{3+} emission were measured upon excitation at 377 and 393 nm. Fig. 4 shows decay curves for Tb^{3+} emission from $^5D_4$ in Tb^{3+} in two concentrated compounds ($Ca_3Tb_2Si_3O_{12}$ and $Ca_3Tb_{1.9}Eu_{0.1}Si_3O_{12}$), and a diluted Tb^{3+} compound ($Ca_{2.97}Tb_{0.03}Y_{1.98}Si_3O_{12}$) to compare the differences in behaviour of this ion. The obtained time constants are reported in Table 1. In the diluted compound there is a clear rise at short times, whereas for the concentrated compounds the curves are well fitted to a single exponential function. This behaviour is explained on the basis of a fast migration regime among the donors, as an effect of the high Tb^{3+} concentration [17,18]. According to Dexter's theory of energy transfer processes through multipolar interaction, the energy transfer probability from a sensitizer to an activator in a dipole–dipole interaction is given by the following formula [19]:

$$P_{sA} = \frac{3\cdot 10^{12} f_d}{R^6 \tau_s} \int \frac{f_s(E) F_A(E)}{E^4} dE \quad (1)$$

where f_d is the oscillator strength of the involved absorption transition of the activator, R is the sensitizer-activator distance, τ_s the radiative decay time for sensitizer, f_s and F_A represent the

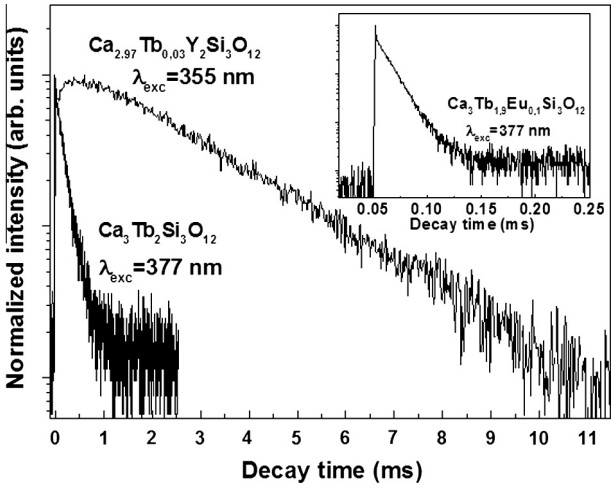

Fig. 4. Room temperature decay curves of the $^5D_4$ Tb^{3+} emission excited at 377 nm in fully Tb-compounds ($Ca_3Tb_{1.9}Eu_{0.1}Si_3O_{12}$) and at 355 nm in a diluted compound ($Ca_{2.97}Tb_{0.03}Y_2Si_3O_{12}$). In the inset is shown the corresponding curve of the $^5D_4$ Tb^{3+} emission excited at 377 nm for $Ca_3Tb_2Si_3O_{12}$.

Table 1
Decay data for the luminescent levels of Tb^{3+} and Eu^{3+} in several oxide hosts upon UV excitation.

Material	Excited state	Decay time (ms)
$Ca_{2.97}Tb_{0.03}Y_2Si_3O_{12}$	$^5D_4$ (Tb^{3+})	2.50 rise + decay
$Ca_3Tb_2Si_3O_{12}$	$^5D_4$ (Tb^{3+})	0.18
$Ca_3Tb_{1.90}Eu_{0.10}Si_3O_{12}$	$^5D_4$ (Tb^{3+})	0.01
$Ca_3Tb_{1.90}Eu_{0.10}Si_3O_{12}$	$^5D_0$ (Eu^{3+})	1.78
$Ca_3Tb_{1.92}Eu_{0.08}Si_3O_{12}$	$^5D_0$ (Eu^{3+})	1.79
$Ca_3Tb_{1.96}Eu_{0.04}Si_3O_{12}$	$^5D_0$ (Eu^{3+})	1.78 small rise + decay
$Ca_3Tb_{1.98}Eu_{0.02}Si_3O_{12}$	$^5D_0$ (Eu^{3+})	1.77 small rise + decay
$Ca_3Eu_2Si_3O_{12}$	$^5D_0$ (Eu^{3+})	0.44

normalized absorption line shape of activator and emission line shape of sensitizer respectively, and E is the energy involved in the transfer. The distance for which the probability of energy transfer equals the probability of a radiative transition is define as the critical distance, and it can be calculated as follows:

$$R_c^6 = 3\cdot 10^{12} f_d \int \frac{f_s(E) F_A(E)}{E^4} dE \quad (2)$$

Using the calculated spectral overlap for $Ca_3Tb_2Si_3O_{12}$ and assuming that for Tb^{3+} transitions the oscillator strength is $3\cdot 10^{-7}$ [20], the critical distance for dipole–dipole energy migration along Tb^{3+} is estimated to be 7.3 Å. It is interesting to compare this with the average Tb–Tb distance, which for nearest neighbours can be calculated with the following formula [21]:

$$d = \left(\frac{3V}{4\pi N}\right)^{1/3} \quad (3)$$

where N is the number of Tb^{3+} atoms in the cell and V is the volume of the cell. The average distance has been found to be 3.14 Å, much smaller than the critical distance for dipole–dipole interaction, so a fast energy migration along Tb^{3+} ions is predicted in this system. This result is in good agreement with the observed behaviour of decay times.

The Tb^{3+} decay constant for the 5%-Eu^{3+} doped sample is significantly shortened respect to the one obtained for $Ca_3Tb_2Si_3O_{12}$. The efficiency of the Tb^{3+}–Eu^{3+} transfer can be calculated according to [22,23]:

$$\eta_T = 1 - \frac{\tau_{Tb-Eu}}{\tau_{Tb}} \quad (4)$$

where τ_{Tb-Eu} and τ_{Tb} are the decay times of Tb^{3+} $^5D_4$ level in the Eu-doped and undoped samples respectively. η_T is found to be 0.94, which indicates that in these conditions the Tb^{3+}–Eu^{3+} energy transfer is very efficient. This value is in good agreement with the results reported by Bettinelli et al. for $Sr_3Tb_{0.90}Eu_{0.10}(PO_4)_3$ (efficiency 0.93) [6], Zhou & Xia for $La_{2.65}GaGe_5O_{12}$:0.15Tb,0.20Eu (efficiency of 0.87) [8] or Xia et al. for $Ba_2Tb_{0.995}(BO_3)_2Cl$:0.005Eu (efficiency of 0.71) [7].

Fig. 5 presents decay curves for Eu^{3+} $^5D_0$ emission for $Ca_3Tb_{2-x}Eu_xSi_3O_{12}$ and $Ca_3Eu_2Si_3O_{12}$ samples. The curves are well fitted by a single exponential function, and the time constants calculated from the decay curves are also reported in Table 1. The exponential profile of the curves is explained on the basis of fast migration among Tb^{3+} and Eu^{3+}, respectively. It is possible to observe that there are no significant changes on decay curves when varying Eu concentration in Eu-doped samples, but the decay is shortened in the case of fully Eu concentrated compound, probably due to concentration quenching as a result of energy migration to quenching impurities. Inset in Fig. 5 presents a zoom on Eu^{3+} decay curves in $Ca_3Tb_{2-x}Eu_xSi_3O_{12}$, in which it is possible to observe a small buildup at short times. This rise is small and hard to identify

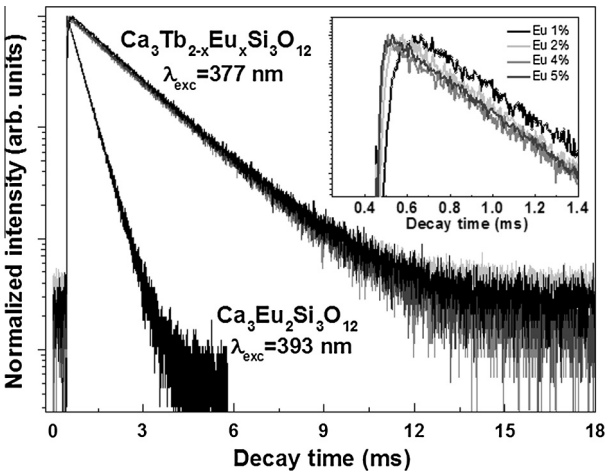

Fig. 5. Room temperature decay curves of the $^5D_0$ Eu^{3+} emission excited at 377 nm ($Ca_3Tb_{2-x}Eu_xSi_3O_{12}$) and 393 nm ($Ca_3Eu_2Si_3O_{12}$).

clearly in the highly-doped samples, indicating that the transfer from Tb^{3+} to Eu^{3+} is fast.

Fig. 6 shows the calculated CIE XYZ chromaticity coordinates diagram for $Ca_3Tb_2Si_3O_{12}$, $Ca_3Tb_{2-x}Eu_xSi_3O_{12}$ and $Ca_3Eu_2Si_3O_{12}$, and a typical picture of the phosphors when excited at 365 nm. As it can be observed, the addition of Eu^{3+} changes the colour emission of the material from green to red, even for low concentrations of activator. The calculated values of CIE coordinates are provided in Table 2.

3.2. Temperature dependent experiments

The temperature evolution in the range 8–330 K of photoluminescence emission and decay time has been studied for $Ca_3Tb_2Si_3O_{12}$ and $Ca_3Tb_{1.9}Eu_{0.1}Si_3O_{12}$. Fig. 7a shows the temperature evolution of decay constant for Tb^{3+} emission at 545 nm upon excitation at 370 nm in $Ca_3Tb_2Si_3O_{12}$. Fig. 7b provides the spectral evolution for Tb^{3+} emission upon the same excitation. The spectrum is dominated by green Tb^{3+} emission at 545 nm, and it is possible to observe a clear decrease of intensity when increasing the temperature of the system, providing an evidence of the previously mentioned energy migration among Tb^{3+} ions. The measured decay curves are approximately exponential, and the obtained values of the decay constants are significantly shorter than the one obtained for an isolated Tb^{3+} ion, which indicates that migration is also present at low temperatures. The evolution of decay time presents a progressive shortening as temperature is increased, until it reaches half of its value when the system is at room temperature. This behaviour is explained because of the disordered nature of the, which provides multiple sites available for Tb^{3+} ions, which implies that the energy migration is not completely resonant and has to be assisted by phonons.

Fig. 8a shows temperature evolution of Tb^{3+} decay time for emission at 540 nm and Eu^{3+} decay time for emission at 611 nm, both for $Ca_3Tb_{1.9}Eu_{0.1}Si_3O_{12}$ phosphor, upon excitation at 370 nm. In Fig. 8b the evolution of the emission spectrum upon excitation at 370 nm is presented. The spectrum is dominated at all temperatures by Eu^{3+} red emission at 611 nm, as observed previously at room temperature, with weak green emission bands coming from

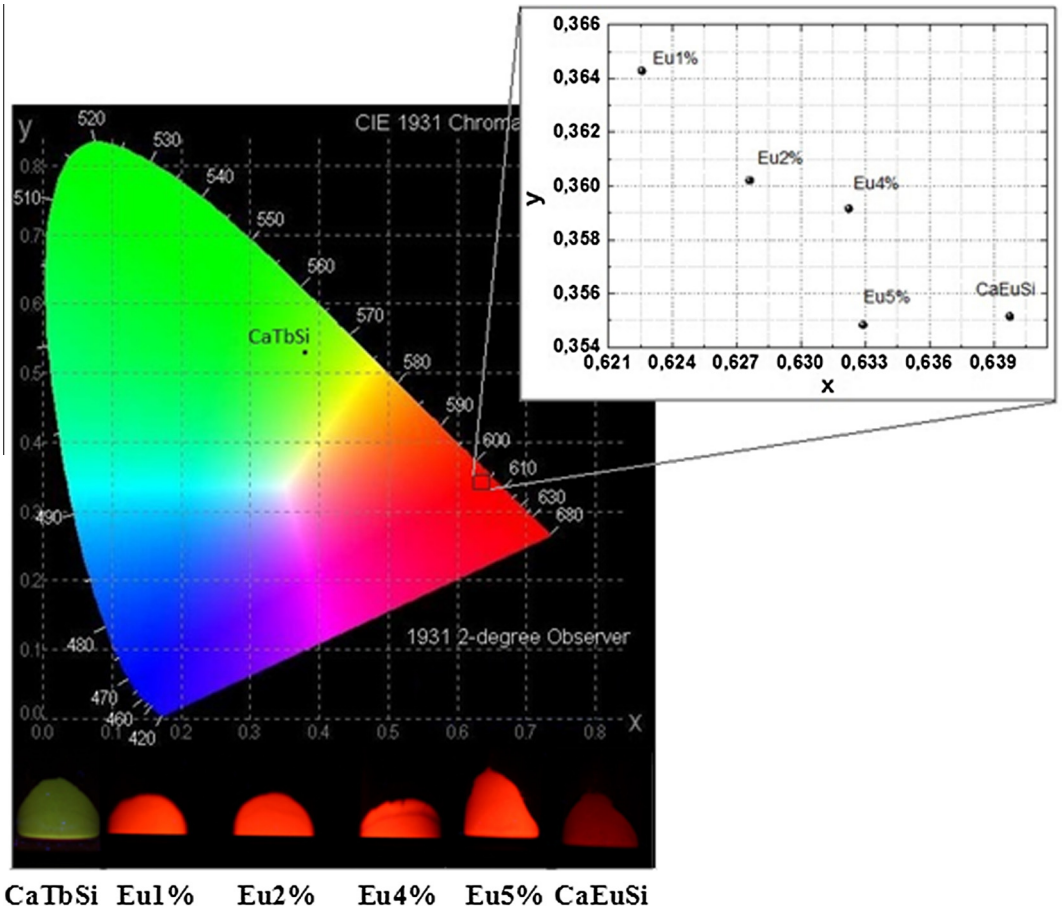

Fig. 6. CIE diagram coordinates of $Ca_3Tb_2Si_3O_{12}$ and $Ca_3Tb_{2-x}Eu_xSi_3O_{12}$ excited at 377 nm and $Ca_3Eu_2Si_3O_{12}$ excited at 393 nm, and typical picture of the phosphors when excited at 365 nm.

Table 2
Calculated values for CIE coordinates of $Ca_3Tb_2Si_3O_{12}$ and $Ca_3Tb_{2-x}Eu_xSi_3O_{12}$ excited at 377 nm and $Ca_3Eu_2Si_3O_{12}$ excited at 393 nm.

Material	*x*	*y*
$Ca_3Tb_2Si_3O_{12}$	0.37716	0.53879
$Ca_3Tb_{1.98}Eu_{0.02}Si_3O_{12}$	0.62257	0.36429
$Ca_3Tb_{1.96}Eu_{0.04}Si_3O_{12}$	0.62760	0.36021
$Ca_3Tb_{1.92}Eu_{0.08}Si_3O_{12}$	0.63223	0.35916
$Ca_3Tb_{1.90}Eu_{0.10}Si_3O_{12}$	0.63290	0.35484
$Ca_3Eu_2Si_3O_{12}$	0.63976	0.35515

Tb^{3+}. The intensity of Eu^{3+} emission bands presents a small reduction as temperature is increased, which could be explained due to phonon-assisted energy migration processes. On the contrary, Tb^{3+} emission is almost quenched due to the combination of the processes of energy migration among Tb^{3+} ions and energy transfer from Tb^{3+} to Eu^{3+}. Decay constant for Eu^{3+} emission does not change significantly in the range studied, while for Tb^{3+} the decay constant is strongly reduced, from 180 μs at low temperature to 12 μs at room temperature. This shortening in time constant is sharp for temperatures up to 60 K, and then decreases slowly. This agrees with the non-resonant nature of the energy transfer, which needs phonons assistance.

Fig. 9 presents the evolution of the efficiency of the energy transfer with temperature. Efficiency values have been calculated from the experimental data using Eq. (4). The efficiency is about 0.50 at low temperatures and rises up to 0.94 at room temperature.

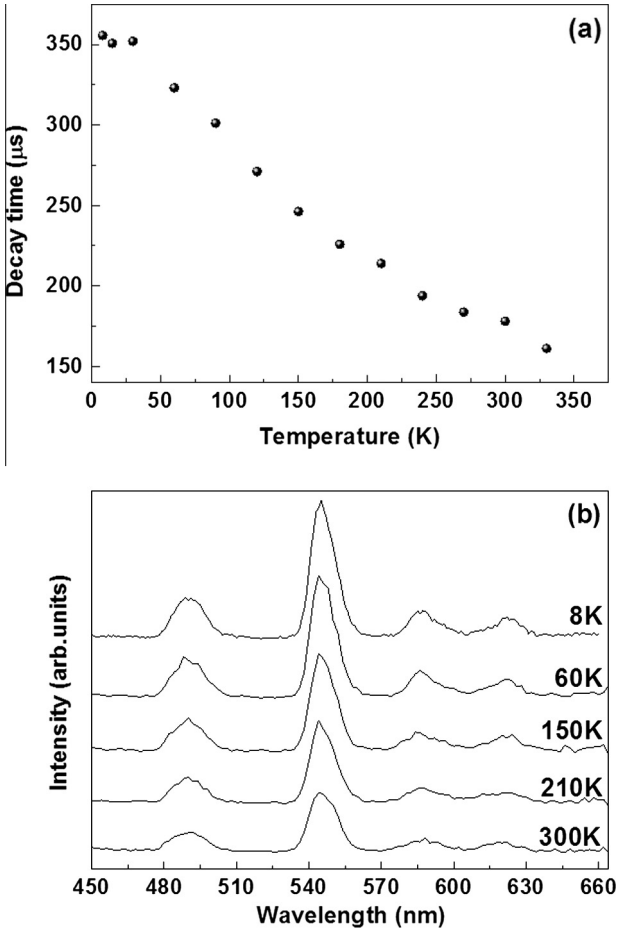

Fig. 7. Temperature evolution in the range 8–330 K upon excitation at 370 nm of Tb^{3+} decay time at 545 nm (a), and Tb^{3+} emission (b). The variation of decay constant is about 55%.

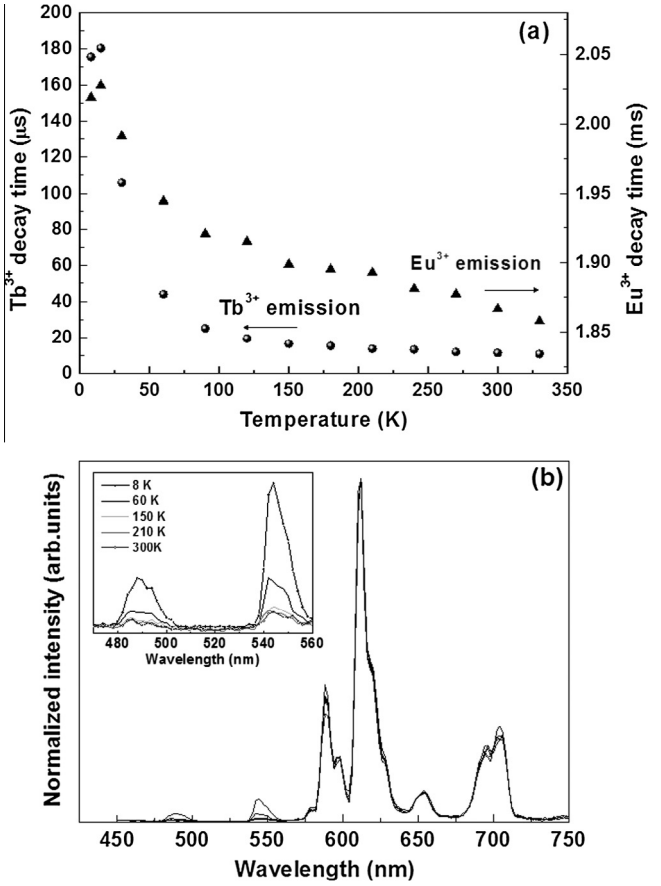

Fig. 8. (a) Temperature evolution in the range 8–330 K of Tb^{3+} decay time at 545 nm (dots) and Eu^{3+} decay time at 611 nm (triangles), upon excitation at 370 nm for $Ca_3Tb_{1.9}Eu_{0.1}Si_3O_{12}$ powders. The variation of decay constant is about 94% for Tb^{3+} and 9% for Eu^{3+}. (b) Evolution of $Ca_3Tb_{1.9}Eu_{0.1}Si_3O_{12}$ emission in the range 8–330 K upon excitation at 370 nm. The spectra are normalized to Eu^{3+} $^5D_0$–$^7F_2$ emission. Inset shows in detail Tb^{3+} emission bands.

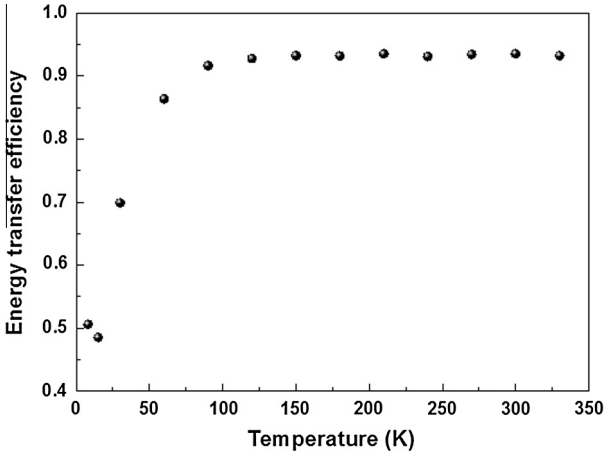

Fig. 9. Temperature evolution in the range 8–330 K of Tb–Eu energy transfer efficiency for $Ca_3Tb_{1.9}Eu_{0.1}Si_3O_{12}$ powders.

This increase takes place rapidly up to 100 K, at which value the efficiency remains stable.

4. Conclusions

In this work the luminescent properties of $Ca_3Tb_2Si_3O_{12}$, $Ca_3Eu_2Si_3O_{12}$ and $Ca_3Tb_{2-x}Eu_xSi_3O_{12}$ powders have been

systematically studied for various Eu^{3+} doping concentration. The temperature evolution of the luminescent properties of $Ca_3Tb_2Si_3O_{12}$ and $Ca_3Tb_{1.9}Eu_{0.1}Si_3O_{12}$ in the range 8–330 K has also been studied. The obtained results show that the addition of Eu^{3+} changes the colour emission of the material from green (Tb^{3+}) to red (Eu^{3+}), evidencing the existence of a very efficient Tb^{3+}–Eu^{3+} energy transfer process. The efficiency of the transfer at room temperature evaluated from the experimental decay times is 0.94 for $Ca_3Tb_{1.9}Eu_{0.1}Si_3O_{12}$, indicating that Tb^{3+} emission is almost quenched while Eu^{3+} emission is enhanced. A fast energy migration process along Tb^{3+} ions is found to be present in fully concentrated Tb^{3+} sample, and it has been observed that this process plays a relevant role in the Tb^{3+}–Eu^{3+} energy transfer, enhancing its efficiency.

Taking all these features into account, it is conceivable to think that it would be possible to synthesize phosphors with intermediate emission colours by adjusting the concentration of Tb^{3+} and Eu^{3+} ions.

Acknowledgments

We would like to thank the European Commission for funding through the Marie Curie Initial Training network LUMINET, grant agreement No. 316906. Expert technical assistance by Erica Viviani (Univ. Verona) is gratefully acknowledged.

References

[1] V.B. Mikhailik, H. Kraus, P. Dorenbos, Phys. Status Solidi RRL 3 (2009) 13.
[2] T. Sheng, Z. Fu, J. Wang, X. Fu, Y. Yu, S. Zhou, S. Zhang, Z. Dai, RSC Adv. 2 (2012) 4697–4702.
[3] C. Ronda, Luminescence. From Theory to Applications, Wiley VCH Verlag GmbH & Co. KGaA, Weinheim, Germany, 2008.
[4] J. Dong, L. Wanga, C. Cuia, Y. Tiana, P. Huang, Ceram. Int. 41 (2015) 1341–1346.
[5] W. Holloway Jr., M. Kestigian, R. Newman, Phys. Rev. Lett. 11 (1963) 458–460.
[6] M. Bettinelli, A. Speghini, F. Piccinelli, J. Ueda, S. Tanabe, Opt. Mater. 33 (2010) 119–122.
[7] Z. Xia, J. Zhuang, L. Liao, Inorg. Chem. 51 (2012) 7202–7209.
[8] J. Zhou, Z. Xia, J. Mater. Chem. C 2 (2014) 6978–6984.
[9] F. Piccinelli, A. Lausi, M. Bettinelli, J. Solid State Chem. 205 (2013) 190–196.
[10] F. Piccinelli, A. Speghini, G. Mariotto, L. Bovo, M. Bettinelli, J. Rare Earths 27 (2009) 555–559.
[11] B. Dickens, W.E. Brown, Tschermaks Mineral. Petrog. Mitt. 16 (1971) 1–27.
[12] G.A. Novak, G.V. Gibbs, Am. Mineral. 56 (1971) 791–825.
[13] F. Piccinelli, A. Lausi, A. Speghini, M. Bettinelli, J. Solid State Chem. 194 (2012) 233–237.
[14] F. Auzel, J. Dexpert-Ghys, D. Morin, G. Dadoun, J. Ostorero, H. Makram, Mater. Res. Bull. 16 (1981) 1521.
[15] J.F.M. dos Santos, I.A.A. Terra, N.G.C. Astrath, F.B. Guimaraes, M.L. Baesso, L.A.O. Nunes, T. Catunda, J. Appl. Phys. 117 (2015) 053102.
[16] G. Blasse, J. Solid State Chem. 2 (1970) 27.
[17] M. Bettinelli, C.D. Flint, J. Phys. Condens. Matter 2 (1990) 8417–8426.
[18] R.K. Watts, Energy Transfer Phenomena, in: B. Di Bartolo (Ed.), Optical Properties of Ions in Solids, Plenum Press, New York and London, 1975, p. 307.
[19] D.L. Dexter, J. Chem. Phys. 21 (5) (1953).
[20] J.M.P.J. Verstegen, J.L. Sommerdijk, J.G. Verriet, J. Lumin. 6 (1973) 425–431.
[21] G. Blasse, J. Solid State Chem. 62 (1986) 207.
[22] J. Pisarska, A. Kos, W.A. Pisarski, Spectrochim. Acta Part A: Mol. Biomol. Spectrosc. 129 (2014) 649–653.
[23] E. Álvarez, M.E. Zayas, J. Alvarado-Rivera, F. Félix-Domínguez, R.P. Duarte-Zamorano, U. Caldiño, J. Lumin. 153 (2014) 198–202.